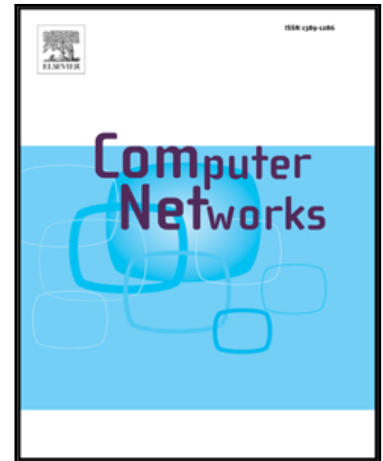


Accepted Manuscript

Optimising Channel Assignment To Prevent Flow Starvation and Improve Fairness For Planning Single Radio WMNs In Built Environments

Ying Qu, Bryan Ng, Michael Homer

PII: S1389-1286(17)30367-5
DOI: [10.1016/j.comnet.2017.09.016](https://doi.org/10.1016/j.comnet.2017.09.016)
Reference: COMPNW 6315



To appear in: *Computer Networks*

Received date: 26 January 2017
Revised date: 1 September 2017
Accepted date: 28 September 2017

Please cite this article as: Ying Qu, Bryan Ng, Michael Homer, Optimising Channel Assignment To Prevent Flow Starvation and Improve Fairness For Planning Single Radio WMNs In Built Environments, *Computer Networks* (2017), doi: [10.1016/j.comnet.2017.09.016](https://doi.org/10.1016/j.comnet.2017.09.016)

This is a PDF file of an unedited manuscript that has been accepted for publication. As a service to our customers we are providing this early version of the manuscript. The manuscript will undergo copyediting, typesetting, and review of the resulting proof before it is published in its final form. Please note that during the production process errors may be discovered which could affect the content, and all legal disclaimers that apply to the journal pertain.

Optimising Channel Assignment To Prevent Flow Starvation and Improve Fairness For Planning Single Radio WMNs In Built Environments

Ying Qu*, Bryan Ng, Michael Homer

*School of Engineering and Computer Science, Victoria University of Wellington, Cotton Building, Gate 6,
Kelburn Parade, Wellington, New Zealand 6140*

Abstract

Wireless mesh networks (WMNs) have many attractive characteristics, such as auto-configuration, self-management, and self-healing. With newer and farther reaching applications being developed in built environments, such as smart grids and intelligent transportation systems, users expect high quality of service and thus fairness is an important issue to be addressed. Channel assignment (CA) is the mechanism for allocating radio resources to the nodes and therefore plays a key role in managing fairness in WMNs. Fairness in WMNs depends on how wireless resources are allocated among the nodes. We examine interference models used in existing CA algorithms and find that CA algorithms using these models yield poor fairness because they only reflect local interference between a link and its interfering links. However, flow starvation is due to network wide interference (i.e. global) involving border links and middle links. We propose a novel anti-starvation channel assignment algorithm (ASCA) for planning single radio WMN. Such ASCA algorithm leverages a new interference model that takes into account both local and global interference. Simulation results show the ASCA algorithm effectively alleviates flow starvation and improves fairness up to 62% compared with the best result from clique-based CA benchmarks. To the best of our knowledge, the

*corresponding author

Email addresses: ying.qu@ecs.vuw.ac.nz (Ying Qu), bryan.ng@ecs.vuw.ac.nz (Bryan Ng), michael.homer@ecs.vuw.ac.nz (Michael Homer)

proposed ASCA is the first one to optimise CA algorithms with consideration of both local and global interference.

Keywords: Wireless Mesh Networks, Channel Assignment, Optimisation, Fairness, Flow starvation, Integer linear programming

1. Introduction

A wireless mesh network (WMN) with a unique “mesh” pattern brings flexible and robust connectivity for various applications, such as providing broadband Internet service for home networks [1–3]. In recent years, some new application scenarios have emerged in WMNs such as smart grids and intelligent transportation systems [4, 5]. The similarity among these applications is that they appear in built environments, such as the central business district or urban living spaces and these environments have a highly structured topology like a line or grid. Since these applications appear in densely populated scenarios, WMNs are expected to provide high quality of service (QoS), such as high Internet speed and fair bandwidth allocation [6–10]. Hence, fairness becomes an important issue to be addressed in WMNs.

Fairness in WMNs depends on how wireless resources are allocated among the nodes in the networks since the relevant resources, such as wireless spectrum, are scarce [2, 11]. If wireless resources are allocated unfairly among the nodes in WMNs, resource starvation can happen and leads to severe QoS degradation [6, 12]. For example, in a large network, when border links are out of each other’s carrier sensing range and these border links dominate the channel transmission causing some middle links to starve [13–16], this occurrence refers to “border effect”. Flow starvation caused by “border effect” in WMNs leads to unfair sharing of a channel among nodes and causes severe degradation in network fairness, which significantly impacts user experience [17–19]. Hence, it is necessary to resolve unfairness problems like flow starvation for improving fairness.

In this paper, we study improving fairness for planning WMNs in built en-

vironments. Fairness in WMNs is defined as the outcome whereby all nodes have fair access to the network, fairly share the channel capacity, and achieve the fair QoS without starvation in the long term. Such fairness in WMNs is measured from the overall network perspective. Improving fairness in WMNs has been studied extensively by using various approaches, such as rate control [20–22], MAC layer enhancement [23–25], or cross-layer design between routing, channel assignment (CA), and scheduling [26–31].

Among these approaches, channel assignment plays a key role in managing fairness of WMNs because it allocates radio resources to the nodes in WMNs [32, 33] and it interfaces the MAC and network layer to ensure fair sharing of channel resources among nodes in WMNs [34–36], which is essential to higher layer protocols. Existing approaches factor in flow starvation in their goals but they did not measure and quantify the efficacy of their designs in resolving flow starvation [20, 21]. Our work in this paper differs from prior work in that we propose a new algorithm that prevents flow starvation and contributes to the debate of the effectiveness of CA algorithms in improving fairness for planning WMNs.

The purpose of this paper is to investigate unfairness problems like flow starvation and solve flow starvation via improved CA algorithms. Our work in this paper is restricted to WMNs using a single radio. However, the insights gained from the evaluation of the single radio WMN can be extended to a multi-radio WMN by considering each radio as an independent overlay WMN. We tackle the fairness problem for WMNs at the design stage (as opposed to the operational and maintenance stage) and thus narrow down the scope to static CA without consideration of traffic pattern. Such a static CA allocates a channel to a node over an extended duration (in terms of weeks or months).

Investigating flow starvation with CA algorithms is closely linked to the interference models. An interference model is embedded within CA algorithms to determine the level of interference between nodes or links. The estimation of interference is used for allocating channels to the nodes in WMNs. One

challenge in CA is to design an interference model to reflect the behaviour in real world applications. An accurate or realistic model directly contributes towards the effectiveness of CA algorithms in estimating interference, eliminating border effect and flow starvation, and achieving desired QoS. Hence, we will examine interference models used by existing CA algorithms and design a new interference model to reflect the behaviour of wireless links in WMNs and thereby eliminate border effect and flow starvation.

The rest of this paper is organised as follows. Section 2 summarises related work and motivates the need for studying unfairness problems with interference models used in CA algorithms. Section 3 introduces the investigation of how different interference models used in CA algorithms influence network fairness and it is premised on some of our earlier work in [37]. Section 4 introduces a new interference model. Section 5 describes the proposed anti-starvation CA algorithm and the validation of this ASCA algorithm through simulation followed by the conclusion in Section 6.

2. Related work

In this section, we will provide a general introduction about the definitions of fairness. Then we discuss how existing CA algorithms set up their objectives related to fairness and interference models used in CA algorithms.

2.1. Fairness definitions

Different definitions of fairness in WMNs have been used in the literature for wireless networks. According to a survey of fairness in [6], fairness can be classified as short-term and long-term fairness, and system and individual fairness. Short-term fairness refers to the resource allocation during a short time period while long-term fairness focuses on the fair resource allocation during a longer time period of the life time of a system. System fairness is observed from the perspective of a whole system regarding the overall fairness among all nodes. Individual fairness shows whether the system treats a certain node fairly according to the traffic demand of this node.

In this paper, we focus on studying long-term and system fairness in WMNs. Our goal is to solve unfairness problems like flow starvation by optimising CA algorithms. Flow starvation is caused by the border effect: that border links keep occupying the channel and some middle links may starve [13–16]. In a
 90 IEEE 802.11 WMN, the border links have fewer conflicting links than the links between borders so the border links are likely to transmit more packets. If border links keep transmitting packets, the transmission attempts of links in the middle have to back off until the channel is released by the border links. Such flow starvation can cause unfair sharing of channel capacity that leads to se-
 95 vere unfairness. Hence, it is necessary to solve flow starvation for improving network fairness in WMNs.

2.2. CA algorithms for fairness

Besides fairness definitions, an important question of fairness is how to make a fair system. Many studies have been conducted to improve fairness
 100 such as rate control [20–22], MAC layer enhancement [23–25], or cross-layer designs between routing, CA, and scheduling [26–31]. However, fairness problems have not been adequately addressed from the aspect of channel reuse and this is an increasingly prevalent problem in dense WMN scenarios under heavy traffic conditions [7, 38–40].

105 A CA algorithm is crucial to network fairness in WMNs because this CA algorithm determines whether radio resource will be allocated fairly among all the nodes. Most CA algorithms maximise overall or average goodput by maximising capacity or mitigating interference [24, 25, 41–61]. These CA algorithms choose the channel with the least co-channel links or the least aggregated traffic load to achieve the highest channel goodput for a given link.
 110

The closest studies to support fairness in CA objectives are [21, 24, 25, 42, 47–49]. Two common fairness metrics used in these CA algorithms are Max-Min fairness (MMF) and proportional fairness (PF). For MMF, the rate of each node or link cannot be increased without decreasing the rate of any other node
 115 or link at the same time in WMNs [21, 24, 25]. The goodput performance of

algorithms targeting MMF is limited by the slowest link. In terms of PF, the studies we surveyed impose a fairness constraint $\lambda = \frac{G_{actual}}{F_{demand}}$ for every node or link, where G_{actual} and F_{demand} denote the actual goodput and the traffic demand. These CA algorithms aim to achieve proportional fairness among flows instead of maximising the overall goodput [42, 47, 49]. Generally, these studies rely on Jain's index in the evaluation of their CA algorithms [54–56] but they did not identify whether flow starvation existed in the first place. Without identifying flow starvation, it is difficult to ascertain whether a CA algorithm resolves flow starvation.

To the best of our knowledge, the study of flow starvation with CA algorithms in WMNs has not received much attention. Therefore, it is necessary to investigate the effectiveness of CA algorithms on solving flow starvation.

2.3. Interference models

As mentioned in the Introduction section of this paper, an interference model is the key element in CA algorithms because CA algorithms use the interference model to estimate interference that directly determines the channel allocation and network fairness. The interference model is specific to a single radio scenario. The overlay strategies for WMNs discussed in [62] appear to be a good fit for extending the single radio interference model to multi radio environment but is beyond the scope of this paper.

Theoretical interference models are widely used in CA algorithms to determine the interference set [24, 25, 41–46, 48–59, 63]. Widely documented theoretical models include protocol model, capture threshold model, and interference range model [64]. No failed packet transmission occurs at a receiver node when its interfering nodes are out of the interference range [65]. Generally, theoretical models only consider the factor of distance and ignore other factors such as transmission power level and the cumulative effect of interfering signals.

Besides theoretical interference models, some CA algorithms use *measurement-based interference models* that are based on the measure of received signal [44, 47]. Measurement-based interference models evaluate interference at a receiver

node by calculating signal-to-interference-and-noise-ratio (SINR) or signal-to-noise-ratio (SNR). When SINR or SNR measured at a receiver node is below a specific threshold, this receiver node probably cannot receive a correct packet and the transmission fails. This assumption is based on massive simulations
 150 for mapping SINR to bite error rate. Note that SINR Threshold is defined based on different modulation and coding mechanisms in different applications [66].

The difference between a theoretical model and a measurement-based model is whether the interference model considers the interference power or the additive effect from multiple neighbouring links or not [64]. Theoretical models assume that interference is a binary or pairwise conflict effect among
 155 concurrent transmitting links without consideration of power and additive effect [64]. Measurement-based models regard interference as an additive effect from all other neighbouring links transmitting simultaneously since SINR calculates the sum of noise signal power and signal power from all interfering
 160 nodes [64]. In summary, theoretical models are simple but not realistic while measurement-based models are realistic but complicated.

Different interference models reflect interference from different perspectives that lead to different channel allocation and fairness in WMNs. In this paper, we investigate whether the theoretical and measurement-based interference models used in CA algorithms can prevent flow starvation. Our study
 165 aims to identify flow starvation in CA algorithms with the help of a new interference model reflecting border effect to optimise CA algorithms. With the new interference model, optimised CA algorithm will resolve flow starvation and improve fairness in WMNs.

170 **3. Investigation of unfairness problems with different interference set selections in CA algorithms**

The main purpose of this section is to investigate unfairness problems by studying how interference models used in existing CA algorithms influence interference set selections and fairness in single radio WMNs. In this paper, we

175 focus on studying the unfairness problem like flow starvation. By exploring the shortcomings of existing interference models, we want to provide guidance to optimise CA algorithms to solve flow starvation and improve network fairness. The unfairness problem in the single radio occurs in multi radio WMNs albeit at a later stage as each radio accommodates more nodes.

180 First, we define three strategies of interference set selections and implement these strategies in a simple clique-based CA algorithm. Second, we run this CA algorithm using different interference set selections in different network topologies. Then we analyse the network fairness of different channel allocations implemented in simulation. Finally, we discuss how flow starvation
185 relates to these interference set selections used by CA algorithms.

We define several variables to facilitate the discussion. The symbols for these variables together appear with a brief explanation in Table. 1.

Table 1: Notation: Symbols and their meanings.

Symbol	Explanation
E	The complete set of links in a WMN
N	The number of links in E
C	The set of available channels for E
P	The topology information of links in E
E_{order}	The set of links in E ordered by a method
R_{cs}	Carrier sensing range
R_I	Interference range
$SIR_{threshold}$	The threshold for Signal-To-Interference Ratio (SIR)
D_{tr}	The distance between a sender and a receiver in the same link
$d_{L,B}$	The distance between a link and the left border link based on the senders' location
$d_{R,B}$	The distance between a link and the right border link based on the senders' location
d_{sr}	The distance between a sender and a receiver from two different links
d_{ss}	The distance between two senders from two different links
d	The inter-link distance interval
D	The distance between two border links based on the senders' location
$\gamma_X(i)$	The interference set of a given link i
β	Path loss exponent factor

3.1. Interference set selections with a clique-based CA algorithm

Here, we introduce the definitions of three interference set selections based
 190 on three distinct interference models and a clique-based CA algorithm. Two
 categories of interference set selection strategies we select are: (i) carrier sensing
 oriented and (ii) packet reception oriented strategies. The carrier sensing
 oriented strategy focuses on the capacity contention between transmitter nodes
 while the packet reception oriented strategy pays particular attention to the in-
 195 terference at a receiver node from neighbouring nodes during the packet recep-
 tion. With the carrier sensing oriented strategy, we define γ_A as carrier sensing
 oriented interference set. For the packet reception oriented strategy, we define
 two distinct interference sets, γ_B and γ_C . The definitions of these interference
 sets are listed below:

200

3.1.1. Carrier sensing oriented strategy

Definition 1. Interference set γ_A

Let E denote the complete set of links in a WMN. For a tagged link i in E , the interference set,

$$\gamma_A(i) = \{l \in E \setminus \{i\} \mid d_{s,s} \leq R_{cs}\}, \quad (1)$$

205 whereby $d_{s,s}$ is the distance between the sender nodes of link l and link i , $d_{s,r}$ is the
 distance between the sender of link l and the receiver of link i , R_{cs} is the carrier sensing
 range.

3.1.2. Packet reception oriented strategies

Definition 2. Interference set γ_B

210 Let E denote the complete set of links in a WMN. For a tagged link i in E , the interference
 set,

$$\gamma_B(i) = \{l \in E \setminus \{i\} \mid d_{s,r} \leq R_I\}, \quad (2)$$

whereby $d_{s,r}$ is the distance between the sender of link l and the receiver of link i , R_I is
 the theoretical interference range ($R_I = k \times D_{tr}, k > 0$).

Definition 3. Interference set γ_C

215 Let E denote the complete set of links in a WMN. For a tagged link i in E , the interference set,

$$\gamma_C(i) = \left\{ l \in E \setminus \{i\} \mid \left(\frac{d_{s,r}}{D_{tr}} \right)^\beta \leq SIR_{thre} \right\}, \quad (3)$$

whereby $d_{s,r}$ is the distance between the sender of link l and the receiver of link i , D_{tr} is the transmitter-receiver separation of link i , β is the path loss exponent factor, SIR_{thre} is the SIR threshold for a successful transmission subject to the used modulation and coding scheme.

220

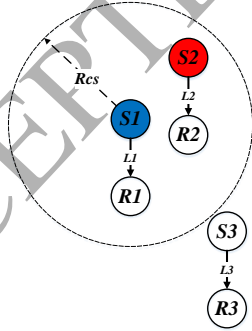
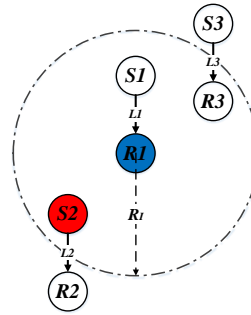
3.1.3. Example: Selecting interference sets

To help understand the difference between three different interference set selection strategies, we use Figure 1 and 2 to demonstrate the selections of these interference sets. The node highlighted in red is in conflict with the node in blue assuming both nodes use the same channel.

225

Carrier sensing oriented interference set γ_A mainly focuses on the capacity contention between sender nodes when they attempt to transmit packets concurrently. In Figure 1, according to Definition 1 of interference set γ_A , $\gamma_A(L1) = \{L2\}$ because sender $S2$ of link $L2$ is within the carrier sensing range of sender $S1$ in link $L1$.

230

Figure 1: Visualising interference set γ_A Figure 2: Visualising interference set γ_B

The packet reception oriented interference sets γ_B and γ_C focus on the po-

tential interference at the receiver node during the packet reception from its sender. The interference sets given by γ_B is based on a theoretical interference model while the interference set γ_C is based on the measurement-based interference model. In Figure 2, $\gamma_B(L1) = \{L2\}$ because sender $S2$ of link $L2$ is
 235 within the interference range R_i of receiver $R1$ of link $L1$.

We use Figure 2 to explain the interference set γ_C . Let us select two-ray ground propagation model [67] and IEEE 802.11b 2Mbps in which $\beta = 4$ and $SIR_{thre} = 10$. According to Definition 3, $d_{s,r} \leq 1.78 \times D_{tr}$. In Figure 2, $\gamma_C(L1) =$
 240 $\{L2\}$ if sender $S2$ of link $L2$ is within the interference range $R_i = 1.78 \times D_{tr}(L2)$ of receiver $R1$ of link $L1$.

3.1.4. Clique-based CA algorithm:

We select a standard clique-based CA algorithm INSTC [68] described in Algorithm 1 and integrate the above three interference set selections with this
 245 CA algorithm. The inputs of this algorithm are: (i) available channel set C , (ii) network link set E , and (iii) node position P with fixed R_{cs} , R_I , and SIR_{thre} . The output is the channel allocation of all links in E .

Algorithm 1: Pseudo code for a clique-based CA algorithm

Input : C, E, P

Output: Channel allocation of all the links in E

```

1 begin
2   foreach link  $i \in E$  do
3     | Select  $\gamma_X(i)$  (see Algorithm 2), where  $X \in \{A, B, C\}$ ;
4   end
5    $E_{order} \leftarrow$  links in  $E$  ordered by Algorithm 3;
6   foreach link  $i \in E_{order}$  do
7     | Select the least used channel in  $C$  among the links in  $\gamma_X(i)$ ;
8   end
9 end

```

Algorithm 2: Constructing interference set $\gamma_X(i)$

```

1  foreach link  $i \in E$  do
2    foreach link  $j \in E \setminus \{i\}$  do
3      switch  $X$  do
4        case  $A$ 
5          if  $d_{s,s} \leq R_{cs}$  then
6             $\gamma_A(i) \leftarrow j$ 
7          end
8        end
9        case  $B$ 
10         if  $d_{s,r} \leq R_I$  then
11            $\gamma_B(i) \leftarrow j$ 
12         end
13       end
14       case  $C$ 
15         if  $(\frac{d_{s,r}}{D_{tr}})^\beta \leq SIR_{thre}$  then
16            $\gamma_C(i) \leftarrow j$ 
17         end
18       end
19     endsw
20   end
21 end

```

Algorithm 1 has three main steps: (i) selecting the interference set for each link in E , (ii) ordering links, and (iii) allocating channels to links in E_{order} . In the first step (in lines 2 – 4 of Algorithm 1), the CA algorithm selects the interference set of each link i as γ_X where $X \in \{A, B, C\}$ denotes the different strategies listed in Algorithm 2. In the second step, the link set E_{order} is sorted in a non-increasing order of the Link Potential Interference (LPI) that is defined as the number of links within the interference set (line 5 of Algorithm 1). We

Algorithm 3: Ordering E based on LPI

```

1 for  $i \leftarrow 1$  to  $N$  by 1 do
2   for  $j \leftarrow 1$  to  $N - i$  by 1 do
3     if  $|\gamma_X(E(j))| \leq |\gamma_X(E(j+1))|$  then
4       temp =  $E(j)$ ;
5        $E(j) = E(j+1)$ ;
6        $E(j+1) = temp$ ;
7     end
8   end
9 end

```

255 select a simple bubble sorting algorithm in Algorithm 3 defined in INSTC [68].
 Next, the CA algorithm allocates channels to the links in the ordered E_{order}
 (lines 6 – 8 of Algorithm 1). The channel allocation strategy is such that the
 least frequently used channel within the interference set of a link i is allocated
 to this link. Such a channel allocation strategy has been widely used in CA
 260 algorithms to reduce the interference among the links within an interference
 set.

3.1.5. Example for the CA algorithm using different interference sets

We execute the CA algorithm given by Algorithm 1 in a WMN deployed
 over a grid topology as an example of applications in built environments. The
 265 grid topology covers an area of $D = 1000$ m, and has 11 single-hop links with
 a constant interval d of 100 m (see Figure 3). We set C as $\{1, 2, 3\}$, R_{CS} as 700 m,
 R_I as $2 \times D_{tr}^{\max}$ (D_{tr}^{\max} is 427 m), β as 4, D_{tr} as 100 m, and SIR_{thre} as 10 dB. All
 these input parameters are calculated based on the parameters in Table 3.

The result of different interference sets is shown in Table 2. The first row
 270 refers to the link index from $L1$ to $L11$ as shown in Figure 3. The second to
 fourth rows list the channel index allocated to each link with the use of three
 different interference sets. For example, the second row is the channel allo-

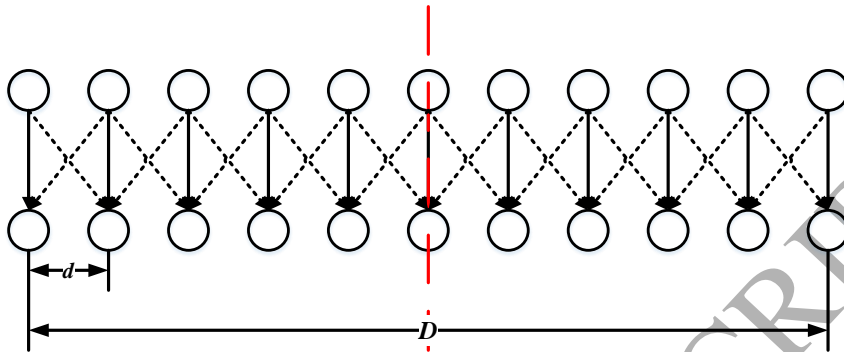


Figure 3: The mesh topology used in Algorithm 1

Table 2: Channel allocations from different interference sets in a 1000×100 m^2 mesh topology

	L_1	L_2	L_3	L_4	L_5	L_6	L_7	L_8	L_9	L_{10}	L_{11}
γ_A	1	2	3	1	2	3	1	2	1	2	3
γ_B	1	2	3	1	2	3	1	2	3	1	2
γ_C	1	2	1	2	1	2	1	2	1	2	1

cation based on interference set selection strategy γ_A . In this table, different interference sets yield different channel allocations.

275 Next, we run the clique-based CA algorithm using three different interference set selections with different network topologies and analyse the fairness among three different interference set selections through simulations.

3.2. Fairness with different interference sets through simulation

In this subsection, we first introduce the inputs of the clique-based CA algorithm such as topologies and the available channel set, simulation configurations, and fairness measures. Then we run the clique-based CA algorithm (see 280 algorithm) in simulation. By analysing the simulation results, we investigate the relationship between flow starvation and three different interference set selections. 285

3.2.1. Algorithm inputs, simulation configuration and fairness measure

The algorithm inputs include available channel set, link set, and network topology. We set the available channel set as $C = \{1, 2, 3\}$ based on IEEE 802.11b protocol that has three non-overlapped channels. The link set ranges from 5 single-hop links to 15 single-hop links. We choose transmitter-receiver separation for all the links in simulation is less than 100 m to guarantee collision-free transmissions (based on the findings from [69]) whereby it was found that carrier sensing mechanism can protect packet transmission against collision when the transmitter-receiver separation is less than $0.56 \times D_{tr}^{\max}$ (D_{tr}^{\max} denotes maximum transmission range).

We select grid and random topologies that range from small border distance $D = 400$ m to large border distance $D = 1400$ m. The grid topologies we use in this section deploy links with a constant interval d of 100 m (see Figure 3). Random topologies we use are generated by a R script. With a given area and given link number, the node position and link length are generated randomly according to uniform distribution. R_{cs} as 700 m, R_I as $2 \times D_{tr}^{\max}$ (D_{tr}^{\max} is 427 m), β as 4, D_{tr} as 100 m, and SIR_{thre} as 10 dB. All these input parameters are calculated based on the parameters in Table 3.

Table 3: Simulation Parameters

Parameter Name	Value
Transmission Power	15 dBm
Receiver Sensitivity	-94 dBm
Path Loss Model	Two-Ray
Shadowing and Fading Model	None
Routing	Static Routing
Physical Layer	IEEE 802.11 b
Data Rate	2 Mbps
Packet Size	1500 Bytes
Inter-packet Interval	6 ms

With the parameters in Table 3, we run the CA algorithm (see Algorithm 1) and implement the channel allocations from the clique-based algorithm into our simulation tool, Qualnet 5.2. The simulation parameters are listed in Table 3. To simplify the analysis, all nodes are identically configured with saturated traffic generators. The average goodput of each links is calculated from 100 randomly seeded simulation runs. All averages shown are reported with confidence interval of 95% with the range from 1.4 to 3.0 kbps under the assumption that the averages are normally distributed.

To evaluate the achieved fairness from simulation results, we select three quantitative fairness measures to investigate the fairness with a certain channel allocation in a WMN. One fairness measure is Jain's index that provides an indication of the overall system fairness [70]. The range of Jain's index is between 0 and 1. The system is fairer when the Jain's index is closer to 1. To further investigate flow starvation, we select another two fairness measures, starvation link ratio and highest-to-lowest goodput ratio [6], because Jain's index does not provide the information about identifying flow starvation. The starvation link ratio that is the ratio between the number of starvation links and the number of all links in a WMN. Starvation link ratio reflects the percentage of starvation links among all links. In this paper, we define the starvation link as that the achieved goodput of a link is less than 20% of the average goodput. Highest-to-lowest goodput ratio is the ratio between the highest achieved goodput and the lowest achieved goodput among all the links in a WMN.

The metrics network goodput and fairness include Jain's index, link starvation ratio, and highest-to-lowest goodput ratio. Their definitions are as follows:

Definition 4. *Jain's index range FI*

Let E denote the set of links in a WMN,

$$FI = \frac{(\sum_{i \in E} G_s(i))^2}{|E| \times \sum_{i \in E} (G_s(i))^2}, \quad (4)$$

where $G_s(i)$ is the normalised goodput of a link i from simulation, $|E|$ is the number of links in E .

Definition 5. Link starvation ratio RS

Let E denote the set of links in a WMN,

$$RS = \frac{|E_{starvation}|}{|E|}, \quad (5)$$

where $|E_{starvation}|$ is the number of links that are predicted to have flow starvation. In this paper, a starvation link is defined as that the achieved goodput of a link is below $\alpha \times G_{average}$, where $\alpha \in [0.0, 0.2]$ is the starvation factor and $G_{average}$ is the average goodput in E . $|E|$ is the number of links in E .

Definition 6. Highest-to-lowest goodput ratio HLG

Let E denote the set of links in a WMN,

$$HLG = \frac{G_{max}}{G_{min}}, \quad (6)$$

where G_{max} and G_{min} are the maximum and minimum goodput values among all links in E respectively.

Next subsection, we will investigate how different interference set selections influence network fairness with different topologies.

3.2.2. Comparison of Jain's index among different interference sets

Figures 4 and 5 are the results of Jain's index from the clique-based CA algorithm using interference set selections γ_A , γ_B , and γ_C in grid and random topologies respectively. In Figure 4 and 5, the X axis denotes the border distance D from 400 m to 1400 m while the Y axis refers to the achieved Jain's index of the channel allocations from different interference sets.

In these two Figures, when border distances D is less than R_{cs} (i.e. 400 m and 600 m, all nodes are within each other's carrier sensing range, so called ideal carrier sensing scenarios), the Jain's indexes of three interference set selections γ_A , γ_B , and γ_C are between 0.75 and 0.98. In grid topologies, γ_C slightly outperforms γ_A and γ_B . In random topologies, γ_A and γ_B achieve better Jain's index than γ_C .

When border distances D is greater than R_{cs} (i.e. between 800 m and 1400 m, not all nodes are within each other's carrier sensing range, so called non-ideal

carrier sensing scenarios), the Jain's indexes from γ_A , γ_B , and γ_C decrease to between 0.4 and 0.7 compared with the results in ideal carrier sensing scenarios. We find one exception that the channel allocation from the interference set γ_A and γ_B achieves 0.95 in the border distance D as 800 m in Figures 4 and 5. The border distance in that random topology is slightly greater than carrier sensing range so that border effect does not exist. In grid topologies, γ_A slightly outperforms γ_B and γ_C . In random topologies, γ_A , γ_B achieve better Jain's index than γ_C .

Overall, the fairness index of three interference set selections decreases with the increase of border distance in grid and random topologies.

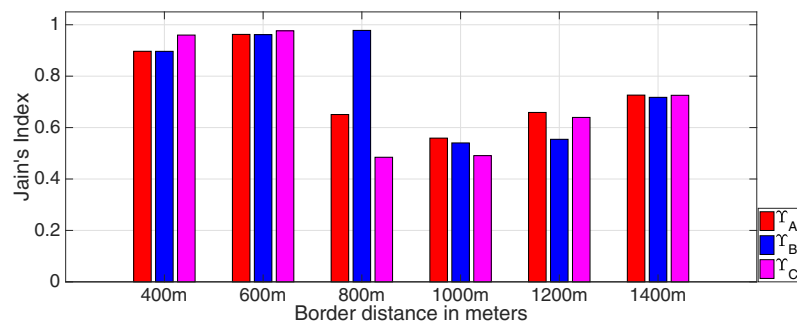


Figure 4: The comparison of Jain's index with different interference sets in grid topologies

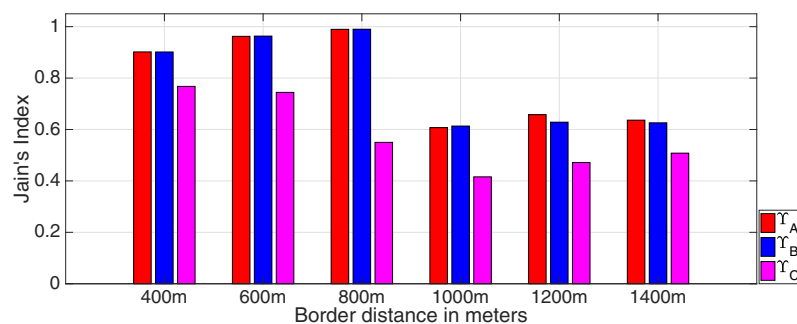


Figure 5: The comparison of Jain's index with different interference sets in random topologies

3.2.3. Comparison of starvation link ratio among different interference sets

Figures 6 and 7 are the results of starvation link ratio from the clique-based
 370 CA algorithm using interference set selections γ_A , γ_B , and γ_C in grid and ran-
 dom topologies respectively. In Figures 6 and 7, the X axis denotes the border
 distance while the Y axis refers to the starvation link ratio of different interfe-
 rence sets. The starvation factor α is assumed as 0.2.

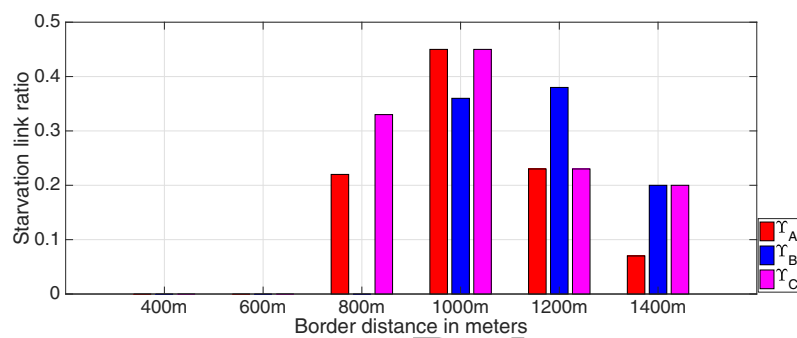


Figure 6: Starvation link ratio with different interference sets in grid topologies

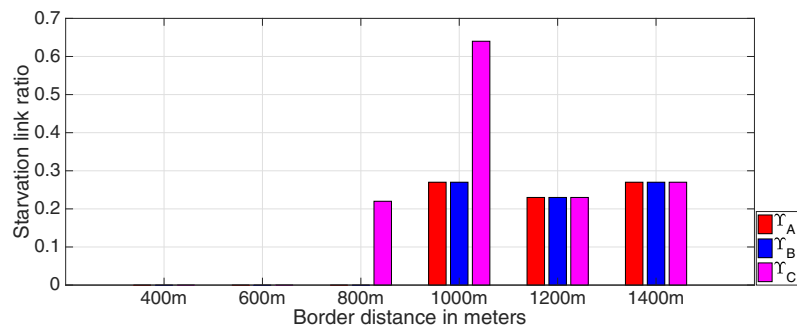


Figure 7: Starvation link ratio with different interference sets in random topologies

375 In these two Figures, when border distance D is less than R_{cs} (i.e. 400 m
 and 600 m, the ideal carrier sensing scenarios), the starvation link ratios of three
 interference set selections γ_A , γ_B , and γ_C are zero, which means flow starvation
 does not exist.

When border distance D is greater than R_{cs} (i.e. between 800 m and 1400 m, the non-ideal carrier sensing scenarios), the starvation link ratio from γ_A , γ_B , and γ_C increases up to 0.65 and decreases. We notice that in the above exceptional case at network size is 800 m in Figures 6 and 7, the channel allocation of interference set γ_A and γ_B experiences no starvation. It explains why the fairness indexes of interference set γ_A and γ_B are higher fairness in 800 m (see Figures 4 and 5). We also notice that the trend of starvation link ratio is opposite to that of Jain's index. The higher starvation link ratio is, the lower Jain's index is.

3.2.4. Comparison of highest-to-lowest goodput ratio among different interference sets

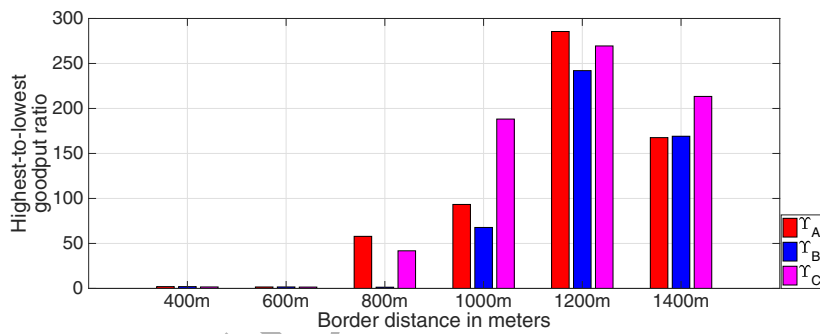


Figure 8: Highest-to-lowest goodput ratio with different interference sets in grid topologies

Figures 8 and 9 are the results of highest-to-lowest goodput ratio from the clique-based CA algorithm using interference set selections γ_A , γ_B , and γ_C in grid and random topologies respectively. In Figures 6 and 7, the X axis denotes the border distance while the Y axis refers to the highest-to-lowest goodput ratio of different interference sets.

In these two Figures, when the border distance D is less than R_{cs} (i.e. 400 m and 600 m, the ideal carrier sensing scenarios), the highest-to-lowest goodput ratios of three interference set selections γ_A , γ_B , and γ_C are very small. When the border distance D is greater than R_{cs} (i.e. between 800 m and 1400 m, the non-ideal carrier sensing scenarios), the highest-to-lowest goodput ratio from

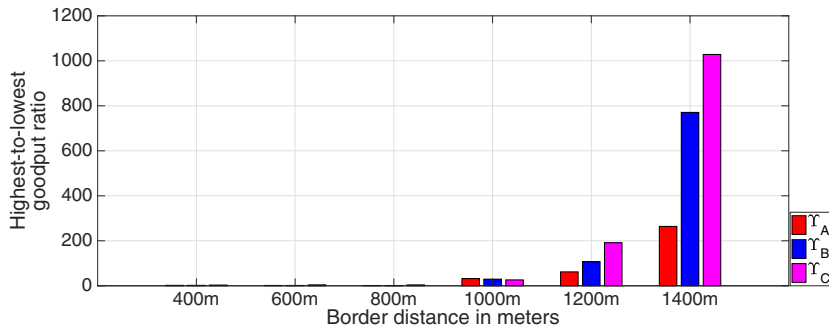


Figure 9: Highest-to-lowest goodput ratio with different interference sets in random topologies

γ_A , γ_B , and γ_C increases up to over 1000. The high highest-to-lowest goodput ratio in Figures 8 and 9 show a different trend compared with the Jain's index in Figures 4 and 5. It matches with our expectation that high highest-to-lowest goodput ratio indicates a low Jain's index.

3.2.5. Jain's index vs. starvation link ratio

To explore the relation between Jain's index and starvation link ratio, we use a scatter plot in Figures 10 and 11. In Figures 10 and 11, the X axis denotes the starvation link ratio while the Y axis refers to the Jain's index. The results in Figure 10 is for a grid topology and Figure 11 for a random topology. In these two figures, when starvation ratio is 0, Jain's index is between 0.75 and 1.0. When starvation ratio increases from 0.06 to 0.64, Jain's index decreases from 0.8 to 0.41. Overall, the greater starvation link ratio, the smaller Jain's index. However, in Figure 10, the points have Jain's indexes around 0.55 but their starvation ratios are quite different. In Figure 11, the points have starvation ratio around 0.24 and their Jain's indexes are much different. Therefore, Jain's index is not sensitive to flow starvation. We will use both metrics to evaluate fairness in this paper.

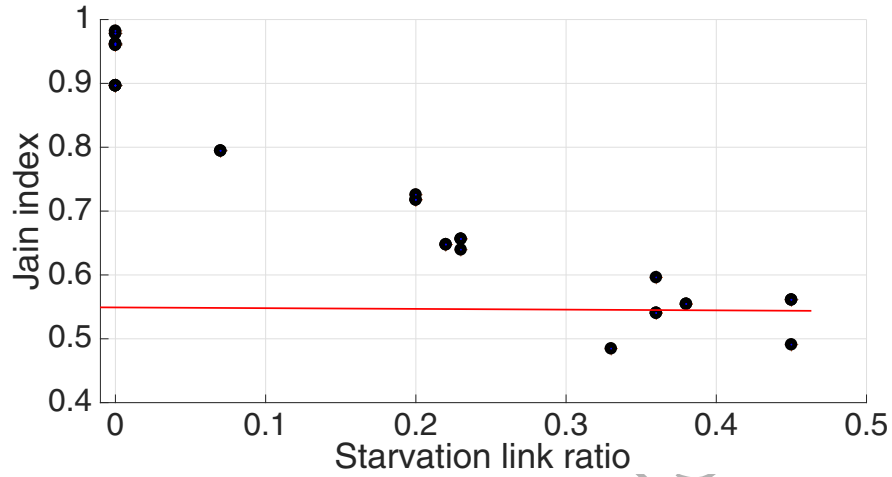


Figure 10: Jain's index vs starvation ratio with different interference sets in grid topologies

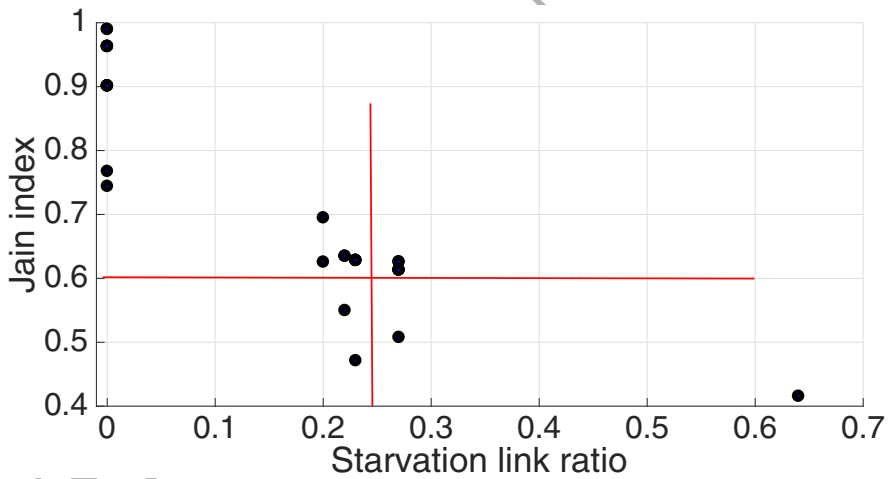


Figure 11: Jain's index vs starvation ratio with different interference sets in random topologies

415 3.3. Flow starvation with interference set selections

Based on the above simulations, we will discuss flow starvation from two main aspects. The first aspect is the network fairness in WMNs under ideal carrier sensing and non-ideal carrier sensing scenarios. Second aspect is the

root cause of flow starvation in non-ideal carrier sensing scenario with respect
 420 to the interference set selection used in CA algorithms.

In the ideal carrier sensing scenarios, channel allocations from all interference
 sets yield high Jain's index. Generally, flow starvation is not observed in
 ideal carrier sensing scenarios so fairness is satisfactory.

In non-ideal carrier sensing scenarios, Jain's index decreases among the
 425 channel allocations from all interference sets due to the occurrence of flow star-
 vation. Overall, the greater starvation link ratio is, the lower Jain's index will
 be. Therefore, we conclude that flow starvation is the reason that causes severe
 fairness degradation in non-ideal carrier sensing scenarios.

Next, we further investigate in non-ideal carrier sensing scenario, why the
 430 existing interference set selections fail to prevent flow starvation and yield poor
 network fairness.

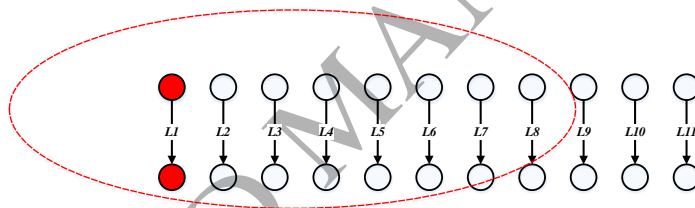


Figure 12: Step 1: allocate a channel to link L_1

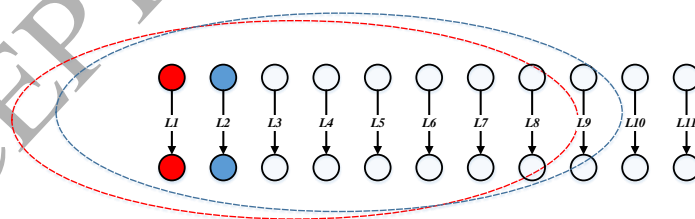
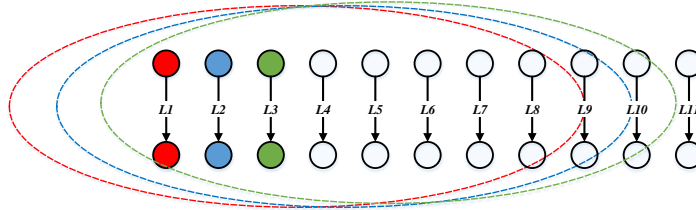


Figure 13: Step 2: allocate a channel to link L_2

We use an example to explore the reason. Figures 12 to 15 show how the
 clique-based CA algorithm using interference set γ_A allocates channels to links

Figure 14: Step 3: allocate a channel to link $L3$

$L1$ to $L11$ in the $1000 \times 100m^2$ topology (See Figure 3). In Figure 12, the CA
 435 algorithm starts from link $L1$ and selects the least-used channel 1 within link
 $L1$'s conflict set as none of the channel has been used before.

In Figure 13, the CA algorithm checks link $L2$'s interference set and selects
 channel 2 because channel 1 has been used. As same as links $L1$ and $L2$, link $L3$
 440 has been allocated with the least used channel 3 (see Figure 14) In the end, all
 the links have been allocated with the least used channel within its interference
 set (see Figure 15).

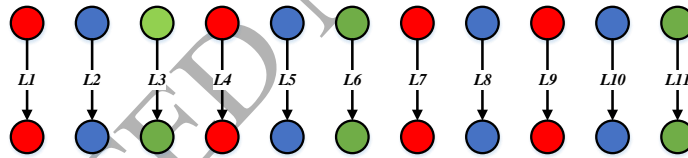


Figure 15: Final step: Channels allocated to all links

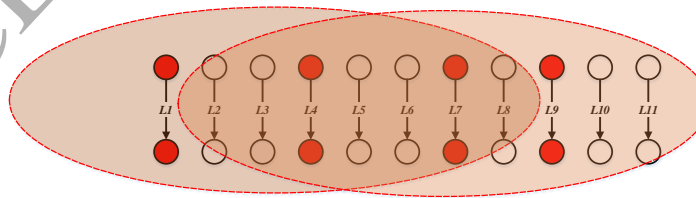


Figure 16: The starvation example in channel 1

In Figure 16, we only list the links allocated with channel 1 from Figure 15. Among all the links using channel 1, links $L1$ and $L9$ are the two border links that are out of each other's carrier sensing range. Hence, border effect exists and causes flow starvation on the middle links $L4$ and $L7$ between two border links. Once starvation exists, the fairness of this WMN degrades significantly.

From these figures, we find that: (i) flow starvation leads to severe unfairness that is caused by global interference between border links and middle links, and (ii) CA algorithms cannot prevent flow starvation because the interference model used to select interference sets only consider local interference between a link and its neighbouring links. Hence, CA algorithms using these interference models result in local optimal solutions. Next section, we will design a new interference model with consideration of both global interference and local interference.

4. A new interference model

In this section, we define a new interference model based on our previous studies [18, 71]. This new interference model reflects two types of interference, local interference and global interference with saturated traffic assumption for the whole network. First, we will explain the definitions of local interference and global interference and then analyse the effect of these two interference on network fairness in WMNs.

4.1. Local interference

In this paper, local interference refers to the interference between a link and its neighbouring links. Such local interference is observed from the perspective of a local node. The three interference set selections in Section 3 are designed based on three local interference models. In our new interference model, we use the local interference model used for selecting γ_A to reflect the local interference. Here, we will not repeat the definition and explain how to select a local interference set.

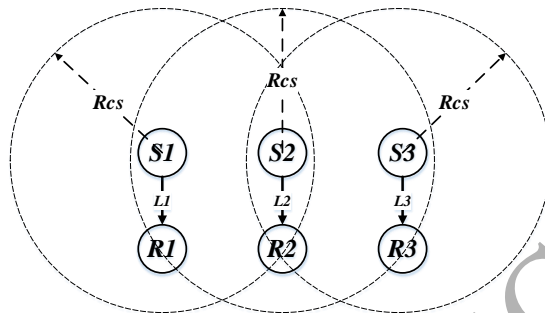


Figure 17: The 3 links scenario

470 4.2. Global interference

Different from the local interference, global interference is observed from the perspective of the whole network and reflects the interference between border links and middle links in a WMN using a single radio when the border links are out of each other's carrier sensing range. The concept of global interference can be extended to a multi radio WMN (with k radios) by assuming each radio has its own global interference set indexed by k . This approach assumes that each of the k radios do not interfere with one another.

Back to the single radio case, for example, Figure 17 is used to explain the concept of global interference. The links $L1$ and $L3$ are the two border links that are beyond each other's carrier sensing range while link $L2$ is in the middle and within the carrier sensing range of both links $L1$ and $L3$. Because border links $L1$ and $L3$ and middle link $L2$ sense the channel state differently, two border links occupy the channel capacity and the middle link get starved under saturated traffic assumption.

485 To help understand the global interference defined in our interference model, we will give the definition of global interference sets and explain how to select global interference sets with an example.

4.2.1. Definition of global interference sets

We define two different types of global interference sets, border sets (γ_{LB} and γ_{RB}) and middle-link set γ_{ML} as follows:

Definition 7. Global interference Border sets γ_{LB} and γ_{RB}

Let E denote the complete set of links in a WMN. For E , the left border set γ_{LB} and the right border set γ_{RB} ,

$$\begin{aligned}\gamma_{LB} &= \{l \in E \setminus \{i \in \gamma_{RB}\} \mid d_{l,i} > R_{cs} \text{ and } F_l < F_i\}, \\ \gamma_{RB} &= \{l \in E \setminus \{i \in \gamma_{LB}\} \mid d_{l,i} > R_{cs} \text{ and } F_l > F_i\}.\end{aligned}\quad (7)$$

whereby $d_{l,i}$ is the Cartesian distance between sender nodes in link l and link i that belong to the left border set and right border set, R_{cs} is the carrier sensing range, F_l and F_i are the Cartesian coordinates of the sender nodes in link l and link i respectively. F is a function extracting either the x or y coordinate of a node, corresponding to the largest dimensions of the bounding box of all nodes in a given network.

Definition 8. Global interference Middle-link set γ_{ML} : Let E denote the complete set of links in a WMN. For E , the middle link set γ_{ML} ,

$$\gamma_{ML} = \{l \in E \setminus \{i \in \gamma_{LB} \text{ or } \in \gamma_{RB}\}\}.\quad (8)$$

4.2.2. Example for selecting global interference sets

We use the topology shown in Figure 18 to illustrate the definitions of global interference set. Based on the Definitions 7 and 8, the interference sets are as follows: $\gamma_{LB} = \{L1, L2\}$, $\gamma_{RB} = \{L10, L11\}$, and $\gamma_{ML} = \{L3 - L9\}$. In Figure 18, two red circles denote the carrier sensing range of γ_{LB} and γ_{RB} . The set of middle links γ_{ML} are defined to be within the carrier sensing ranges of both γ_{LB} and γ_{RB} . γ_{LB} and γ_{RB} are out of each other's carrier sensing range. The global interference sets γ_{LB} , γ_{RB} , and γ_{ML} will be used in our proposed CA algorithm to improve fairness.

4.3. Analysis about the effect of local and global interference on fairness

Based on the above definitions and the investigation in section 3, we will discuss the effect of local interference and global interference on fairness. The

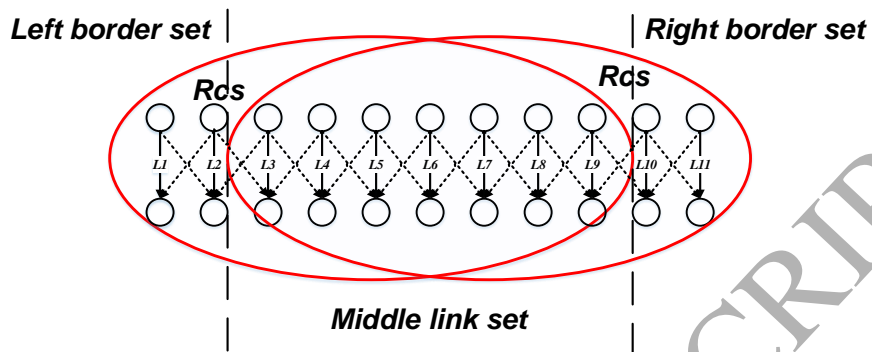


Figure 18: Selecting global interference sets

local interference between a link and its interfering links normally causes the variation of network fairness among these links, while the global interference
 515 between border links and middle links may cause flow starvation that can lead to significant fairness degradation. Therefore, global interference is the main cause of unfairness in WMNs. To improve fairness in WMNs, we need to first solve flow starvation caused by the primary factor, global interference and then alleviate local interference.

520 In next sections, we will validate our analysis by applying our new interference model to a new CA algorithm to select local and global interference sets.

5. Solving flow starvation and improving fairness

525 In this section, we develop a new Anti-Starvation Channel Assignment (ASCA) algorithm to solve the flow starvation problem and improve the fairness among the links in a WMN. We first introduce the design of this ASCA algorithm and then validate ASCA algorithm through simulation compared with the results in Section 3.

5.1. The design of ASCA algorithm

530 Our proposed ASCA algorithm aims to improve fairness by solving global interference and preventing flow starvation. As we mentioned in Section 1, we propose the ASCA as a static and traffic-unaware CA algorithm for planning WMNs.

Figure 19 shows the logic flow of the ASCA algorithm. The input and out-
535 put of Algorithm 4 are identical to those of Algorithm 1. the ASCA algorithm first check whether the border distance D of a given WMN is greater than carrier sensing range R_{CS} . If $D \leq R_{CS}$ that this WMN is an ideal carrier sensing scenario, we apply a partition CA algorithm to allocate channels to the links in the network. The purpose of using a partition CA algorithm is to alleviate in-
540 terference and achieve the fairness among subgroups using different channels. If $D > R_{CS}$ that the given WMN is a non-ideal carrier sensing scenario and global interference may exist, the ASCA algorithm will first solve the global interference and then reduce the local interference among the links within each global interference sets.

545 To solve the global interference in non-ideal carrier sensing scenarios, the ASCA algorithm first identifies the global interference sets and formulates the objective function to achieve the fairness among three global interference sets as an ILP problem in Definition 9. The objective is defined to achieve the maximum fairness by minimising the difference of goodput between the border sets
550 and the middle set. In Definition 9, y is the variable that refers to the number of channels for the border set. M , $|\gamma_B|$, and N are three constant values from CA inputs denoting the number of available channels, the number of links in the border set and the number of links in the whole network respectively.

To achieve fairness among three global interference sets, we try to find a y
555 representing the channel number allocated to the global border sets, which can minimise the difference of average goodput between global border sets and global middle link sets in equation 10 by satisfying the constraint that y is no more than the available channel number M .

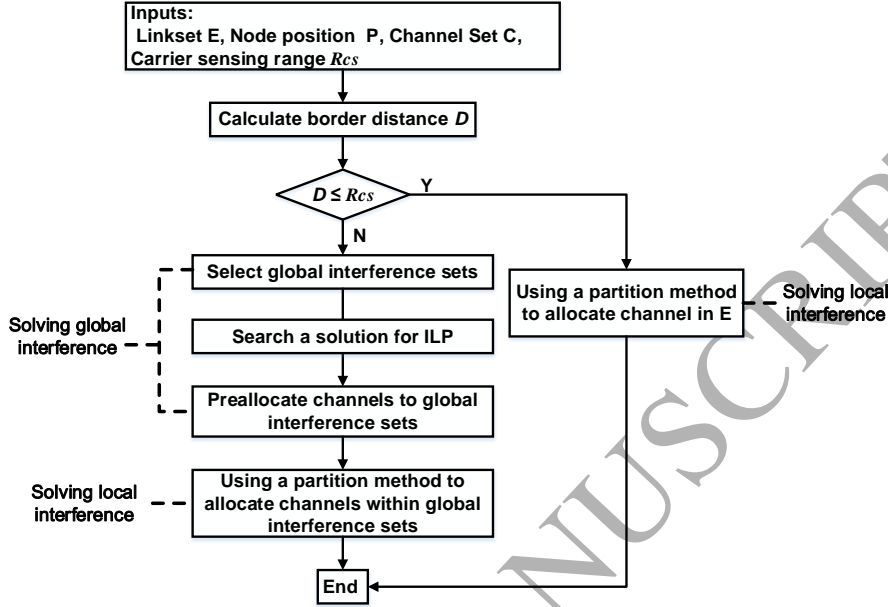


Figure 19: The logic flow of the ASCA algorithm

Definition 9. Objective function: Let E denote the complete set of links in a WMN.

560 The objective is to:

maximise Fairness in E via minimising the expression in 10, (9)

$$\arg \min_{\substack{y \in \mathbb{Z}^+ \\ 0 < y \leq M-1}} \left(\frac{y}{|\gamma_B|} - \frac{M-y}{N-2 \times |\gamma_B|} \right), \quad (10)$$

whereby M is the available channel number, y is the channel number for border sets, γ_B is the link number of one border set, N is the link number in E .

The formulation of the objective function in Definition 9 is essentially an Integer Linear Programming (ILP) problem seeking a y that maximises fairness.

565 Because the objective function has a single variable and is bounded by $M-1$, therefore the complexity of the ILP formulation is $O(M-1)$ where M is the number of available channels [72].

With the solution from the ILP function, the ASCA algorithm preallocates

the channels to the global border sets and middle link set. Our strategy to solve
 570 flow starvation is to allocate distinct channels to global border sets and middle
 set. After that, the ASCA selects a partition method to allocate preallocated
 channels to the links within each global interference set. The purpose of using
 a partition CA algorithm is to achieve the fairness among each links in each
 global interference set.

575 The design of the ASCA is listed in Algorithm 4. First, the ASCA algorithm
 orders with all links within E based on Definition 7 with an increasing order
 (lines 2 of Algorithm 4). In line 3 of Algorithm 4, the ASCA algorithm calcu-
 lates the network size D . If border distance $D \leq R_{CS}$ (an ideal carrier sensing
 scenario), the ASCA algorithm uses a partition method in Algorithm 6 to di-
 580 vide link set E into subgroups based on the allocated channel number (see line
 5 of Algorithm 4).

If border distance $D > R_{CS}$ (a non-ideal carrier sensing scenario), the ASCA
 algorithm has two phases for this situation. In the first phase, the ASCA algo-
 rithm selects global interference sets (see lines 7 of Algorithm 4). The logic for
 585 constructing the global interference sets is listed in Algorithm 5 that we first se-
 lect two border sets in E based on the Definition 7 and then adds the remaining
 links to γ_{ML} . Subsequently, the ASCA searches the optimal channel number γ
 to satisfy the ILP objective function in line 8 of Algorithm 4. Then the ASCA se-
 lects distinct channels to global border sets and middle link set (see lines 9 – 10
 590 of Algorithm 4). In the second phase, the ASCA uses the partition method (see
 Algorithm 6) to divide each global interference set into subgroups based on the
 allocated channel number (see line 11 of Algorithm 4).

For non-ideal carrier sensing scenarios, in the first phase, the ASCA algo-
 rithm solves global interference by partitioning border sets and middle-link set
 595 with different channels and allocates identical channel to γ_{LB} and γ_{RB} to im-
 prove spatial reuse while in the second phase, the ASCA algorithm minimises
 local interference within each global interference set.

In the ASCA algorithm, we select a simple partition method (c.f. Algo-
 rithm 6). In Algorithm 6, the inputs are the link set $E_{reorder}$ and the avail-

Algorithm 4: Pseudo code for the ASCA algorithm**Input** : C, E, P **Output:** Channel allocation of all the links in E

```

1 begin
2    $E_{reorder} \leftarrow$  links in  $E$  sorted with an increasing order based on
   Definition 7 ;
3   Calculate  $D = |E_{reorder}[last] - E_{reorder}[first]|$ ;
4   if  $D \leq R_{cs}$  then
5     Apply a partition algorithm to  $E_{reorder}$  (see Algorithm 6);
6   else
7     Select  $\gamma_{LB}$ ,  $\gamma_{RB}$ , and  $\gamma_{ML}$  (see Algorithm 5) ;
8     Calculate  $y$  to achieve  $\min \left( \frac{y}{|\gamma_B|} - \frac{M-y}{N-2 \times |\gamma_B|} \right)$ ;
9     Randomly select channels  $y \in C$  to  $\gamma_{LB}$  and  $\gamma_{RB}$ ;
10    Select channels  $Z \in C \setminus \{y\}$  to  $\gamma_{ML}$ ;
11    Apply a partition algorithm to  $\gamma_{LB}$ ,  $\gamma_{RB}$ , and  $\gamma_{ML}$  (see
    Algorithm 6);
12  end
13 end

```

Algorithm 5: Selecting global interference sets γ_{LB} , γ_{RB} , and γ_{ML}

```

1 foreach link  $i \in E_{reorder}$  do
2   Select link  $j = E_{reorder}[last]$ ;
3   if  $d_{i,j} > R_{cs}$  then
4      $\gamma_{LB} \leftarrow i$ 
5   end
6 end
7 foreach link  $i \in E_{reorder}$  do
8   Select link  $j = E_{reorder}[first]$ ;
9   if  $d_{i,j} > R_{cs}$  then
10     $\gamma_{RB} \leftarrow i$ 
11  end
12 end
13 foreach link  $i \in \gamma_{LB}$  do
14   foreach link  $j \in \gamma_{RB}$  do
15     if  $d_{i,j} \leq R_{cs}$  then
16       Remove link  $i$  from  $\gamma_{LB}$ ;
17       Remove link  $j$  from  $\gamma_{RB}$ ;
18       Go to 13;
19     end
20   end
21 end
22 foreach link  $i \in E_{order}$  do
23   if link  $i \notin \gamma_{LB} \cup \gamma_{RB}$  then
24      $\gamma_{ML} \leftarrow i$ 
25   end
26 end

```

Algorithm 6: Pseudo code for a partition CA algorithm

Input : C, E

Output: Channel allocation of all the links in E

```

1 begin
2   Divide  $E$  into subsets  $E(i)$ , indexed by channel index  $i \in C$ ;
3   foreach Channel  $i \in C$  do
4     Allocate channel  $i$  to  $E(i)$ ;
5   end
6 end

```

able channel set C and output is the channel allocation of the links in E_{order} . This partition CA algorithm divides the link set $E_{reorder}$ into groups where the number of groups is equal to the number of available channels (line 2 of Algorithm 6) and allocate each group with different channels (lines 3 – 5 of Algorithm 6). By using different channels in different groups, the partition CA algorithm mitigates the channel contention among different groups.

5.2. Validation of the ASCA algorithm with three channels

In this subsection, we validate the ASCA algorithm with our benchmarks through simulation. Our benchmarks are the clique-based algorithm with three different interference set selections γ_A , γ_B , and γ_C (see Section 3) and single-channel (SC) CA algorithm. The algorithm inputs and simulation configurations are as same as those in section 3.2.1. We validate our ASCA algorithm from four aspects, overall Jain's index, starvation link ratio, highest-to-lowest goodput ratio and average goodput.

5.2.1. Comparison of Jain's index

Figure 20 and 21 are the results of Jain's index from the clique-based CA algorithm using interference set selections γ_A , γ_B , and γ_C , SC CA algorithm, and ASCA algorithm in grid and random topologies respectively. In Figures 20 and 21, the X axis denotes the border distance in Figure 3 from 400 m to 1400 m

while the Y axis refers to the achieved Jain's index of the channel allocations from different algorithms.

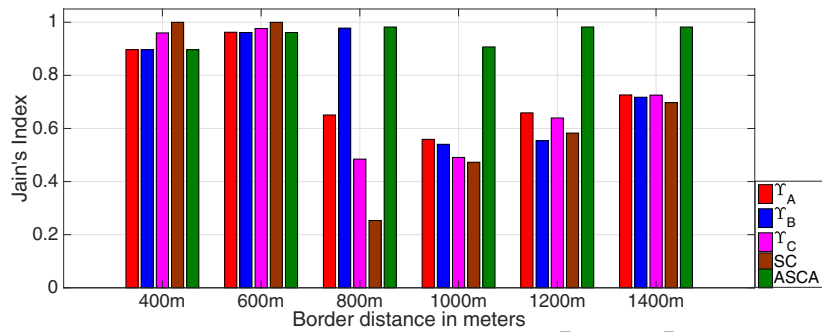


Figure 20: The comparison of Jain's index using three channels in grid topologies

620

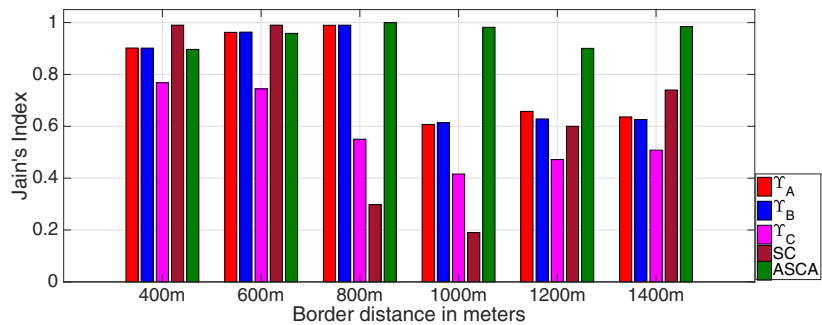


Figure 21: The comparison of Jain's index using three channels in random topologies

In these two Figures, when the border distance is less than R_{cs} (i.e. 400 m and 600 m, the ideal carrier sensing scenarios), all five CA algorithms achieve similar Jain's index. When the border distance is greater than R_{cs} (i.e. between 800 m and 1400 m, the non-ideal carrier sensing scenarios), the ASCA algorithm achieves better Jain's index than other four CA algorithms in both grid and random topologies. We also notice that in non-ideal carrier sensing scenarios, the clique-based CA algorithm using three available channels achieves the

625

similar Jain's index as that of SC CA algorithm. It shows that more available channels may not contribute to high fairness if the CA algorithm cannot effectively prevent flow starvation. Overall, in non-ideal carrier sensing scenarios, the ASCA algorithm achieves 24–62% better fairness compared with the selection strategy γ_A (the highest among three interference sets) in terms of Jain's index.

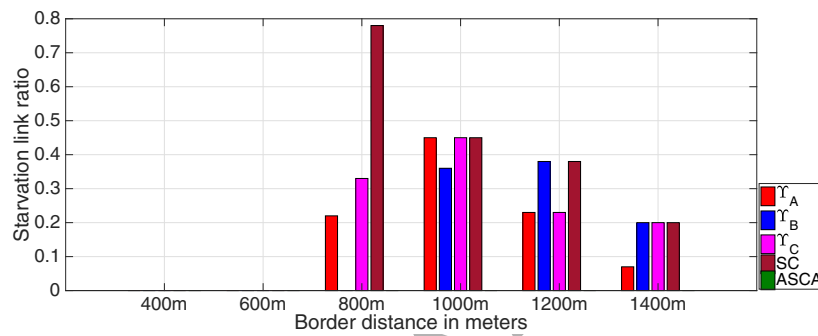


Figure 22: The comparison of starvation link ratio using three channels in grid topologies

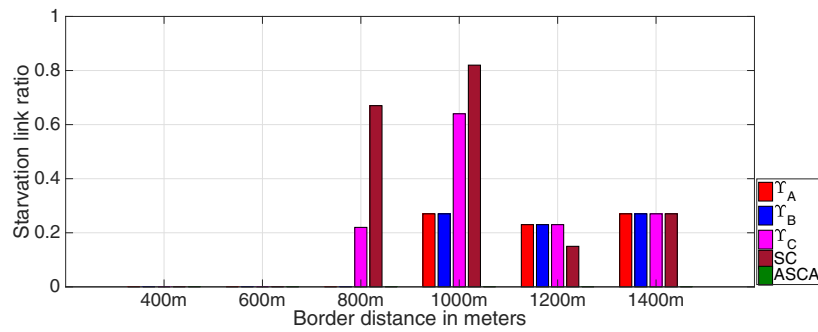


Figure 23: The comparison of starvation link ratio using three channels in random topologies

5.2.2. Comparison of starvation link ratio

Figures 22 and 23 are the results of starvation link ratio from the clique-based CA algorithm using interference set selections γ_A , γ_B , and γ_C , SC CA

algorithm, and ASCA algorithm in grid and random topologies respectively. In Figure 22 and 23, the X axis denotes the border distance in Figure 3 while the Y axis refers to the starvation link ratio of different CA algorithms. The starvation factor α is assumed as 0.2.

In these two Figures, when the border distance is less than R_{cs} (i.e. 400 m and 600 m, the ideal carrier sensing scenarios), the starvation link ratios of all CA algorithms are zero, which means starvation does not exist. When the border distance is greater than R_{cs} (i.e. between 800 m and 1400 m, the non-ideal carrier sensing scenarios), only ASCA algorithm remains the starvation link ratio as zero while flow starvation exists in the channel allocation of other CA algorithms. The zero starvation link ratio of ASCA algorithm explains the corresponding high Jain's index in Figures 20 and 21.

5.2.3. Comparison of highest-to-lowest goodput ratio

Figures 24 and 25 are the results of highest-to-lowest goodput ratio from the clique-based CA algorithm using interference set selections γ_A , γ_B , and γ_C , SC CA algorithm, and ASCA algorithm in grid and random topologies respectively. In Figures 24 and 25, the X axis denotes the border distance in Figure 3 while the Y axis refers to the highest-to-lowest goodput ratio of different CA algorithms.

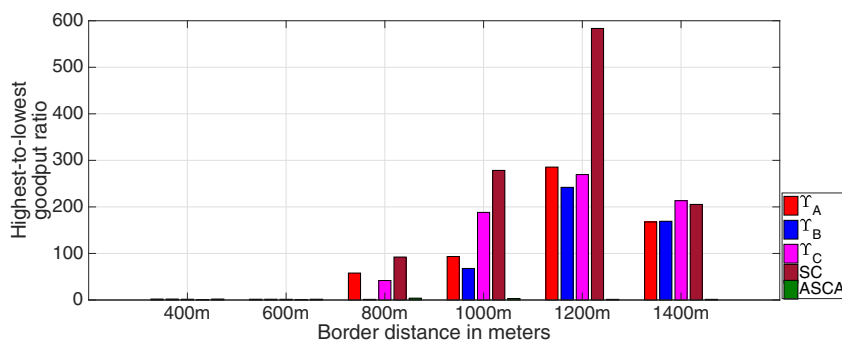


Figure 24: The comparison of highest-to-lowest goodput ratio using three channels in grid topologies

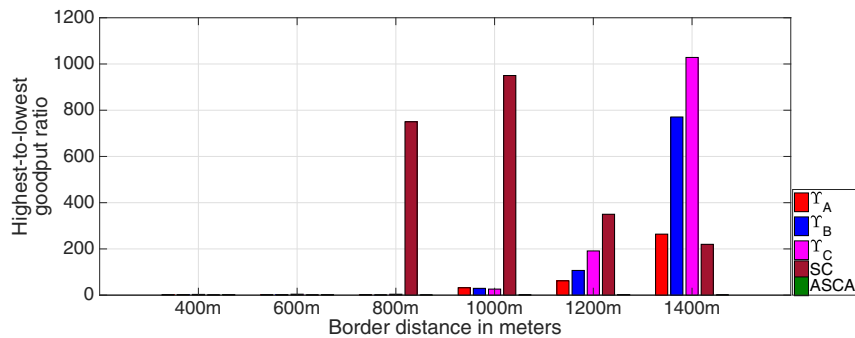


Figure 25: The comparison of highest-to-lowest goodput ratio using three channels in random topologies

655 In these two Figures, when the border distance is less than R_{CS} (i.e. 400 m and 600 m, the ideal carrier sensing scenarios), the highest-to-lowest goodput ratios of all CA algorithms are very small. When the border distance is greater than R_{CS} (i.e. between 800 m and 1400 m, the non-ideal carrier sensing scenarios), the highest-to-lowest goodput ratio of the ASCA algorithm remains very
660 small compared with the other four algorithms.

5.2.4. Comparison of average goodput

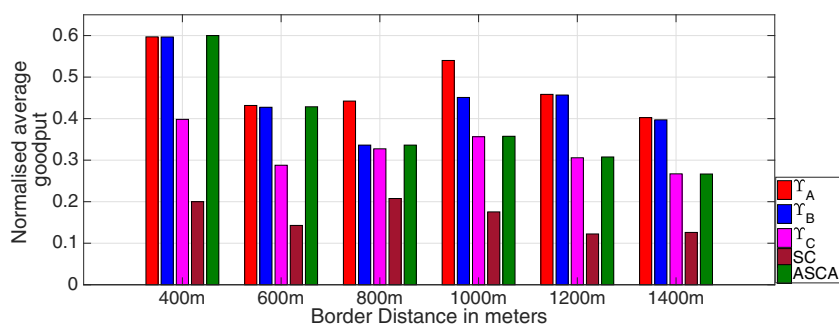


Figure 26: The comparison of average goodput using three channels in grid topologies

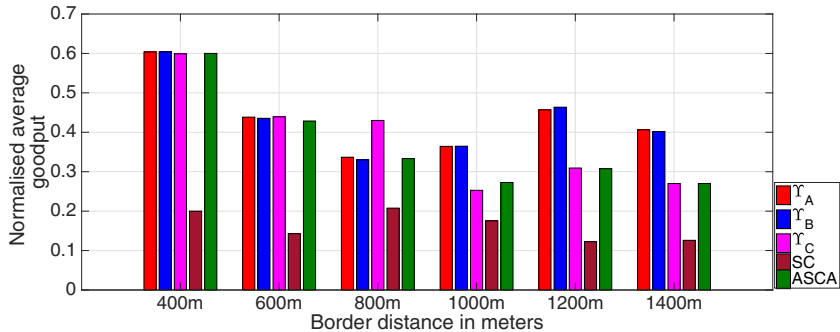


Figure 27: The comparison of average goodput using three channels in random topologies

To further evaluate the performance of the ASCA algorithm, we compare the ASCA algorithm with the other four CA algorithms in terms of average goodput. Figures 26 and 27 are the results of average goodput from the clique-based algorithm using interference set selections γ_A , γ_B , and γ_C , SC CA algorithm, and ASCA algorithm in grid and random topologies respectively. In Figures 26 and 27, the X axis denotes the border distance in Figure 3 while the Y axis refers to the average goodput of different CA algorithms.

In these two Figures, when the border distance is less than R_{cs} (i.e. 400 m and 600 m, the ideal carrier sensing scenarios), the ASCA algorithm achieves the same average goodput as that of the clique-based CA algorithm using γ_A and γ_B . SC CA algorithm achieves least average goodput. When the border distance is greater than R_{cs} (i.e. between 800 m and 1400 m, so called non-ideal carrier sensing scenarios), the ASCA algorithm decreases 24–34% in average goodput compared with the best result from γ_A . The reason for γ_A and γ_B achieving higher goodput than ASCA is that γ_A and γ_B reuse all the channels in the non-ideal carrier sensing scenarios. But the ASCA algorithm partially reuses the channels to eliminate border effect and flow starvation that scarifies the average goodput.

680 5.3. Validation of ASCA algorithm with twelve channels

In this subsection, we validate the ASCA algorithm with our benchmarks using twelve channels through simulation. The grid topologies we use in this subsection deploy links with $D = 1000m$, $D_{tr} = 50m$ and constant interval d of 30 m (see Figure 3). The simulation configurations is in Table 4. The number of 685 available channels is 12 and the carrier sensing range is 675 m according to the configuration in Table 4. We validate our ASCA algorithm from four aspects, overall Jain's index, starvation link ratio, highest-to-lowest goodput ratio and average goodput. The starvation factor α is assumed as 0.2.

Table 4: Simulation Parameters

Parameter Name	Value
Transmission Power	20 dBm
Receiver Sensitivity	-85 dBm
Path Loss Model	Two-Ray
Shadowing and Fading Model	None
Routing	Static Routing
Physical Layer	IEEE 802.11 a
Data Rate	6 Mbps
Packet Size	1500 Bytes
Inter-packet Interval	2 ms

In Figure 28, the ASCA algorithm achieves the highest Jain's index among 690 all CA algorithms. Even using 12 channels in such a dense topology, the clique-based CA algorithm using interference set selections γ_A , γ_B , and γ_C still have flow starvation but ASCA algorithm effectively prevents flow starvation (see Figure 29). This shows that existing interference models still drive CA algo- 695 rithm to flow starvation and poor fairness with more channels available because they only consider local interference.

Figure 30 shows that the ASCA algorithm outperforms the other CA algorithms in terms of highest-to-lowest goodput ratio. This matches with the

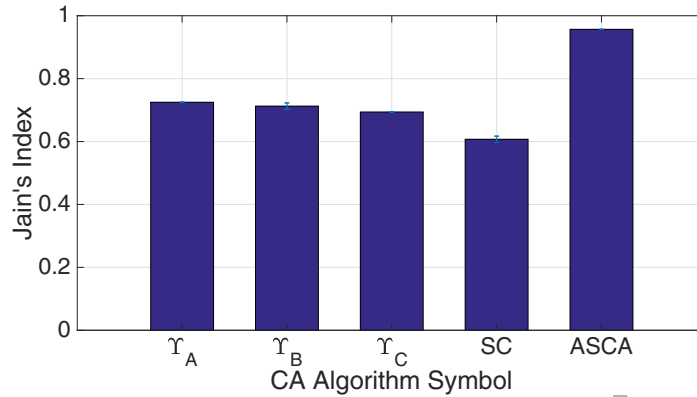


Figure 28: The comparison of fairness index using twelve channels in a grid topology

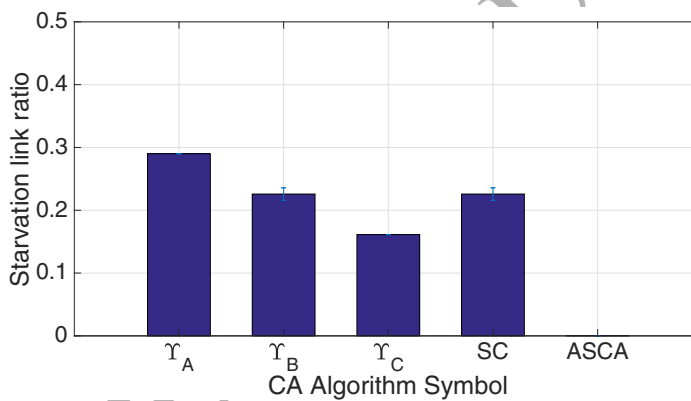


Figure 29: The comparison of starvation ratio using twelve channels in a grid topology

Jain's index trend in Figure 28. For average goodput, the ASCA algorithm achieves more than γ_C and SC but γ_A and γ_B achieves higher goodput than ASCA. Along the same lines of explanation in Section 5.2.4, γ_A and γ_B fully reuse the 12 available channels for the links in the topology but the ASCA algorithm partially reuse these channels to separate border sets and middle sets with different channels that sacrifices average goodput. The interference set γ_C select fewer channels the selection strategy and SC has only one available channel.

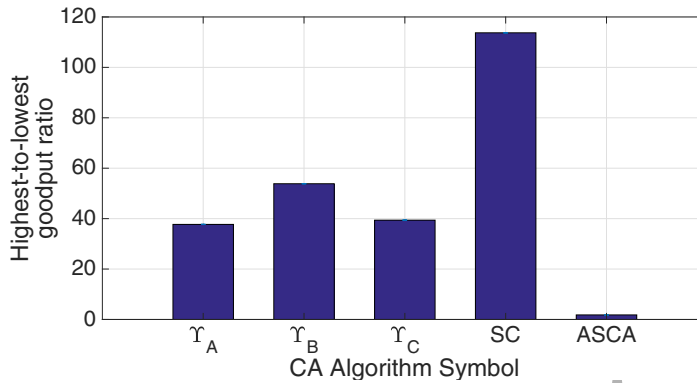


Figure 30: The comparison of high-to-low goodput ratio using twelve channels

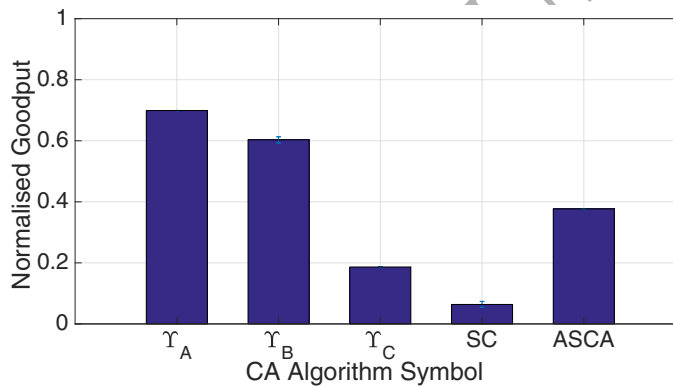


Figure 31: The comparison of average goodput using twelve channels

5.4. Discussion about ASCA algorithm

In this section, we propose a CA algorithm (ASCA) to solve flow starvation and improve fairness in WMNs. Through simulation validation, we find that in ideal carrier sensing scenarios, the ASCA algorithm achieves similar fairness and average goodput as the clique-based CA algorithm using interference set selections γ_A , γ_B , and γ_C . It matches with our expectation that flow starvation does not exist in ideal carrier sensing scenarios and all links fairly share the channel capacity.

In non-ideal carrier sensing scenarios, the ASCA algorithm achieves highest
 715 fairness among all the CA algorithms by preventing flow starvation. However,
 it attains lower average goodput compared with the clique-based CA algo-
 rithm using interference set selections γ_A and γ_B . To prevent flow starvation
 and improve fairness, our algorithm partitions the border sets and middle-link
 set with different channel, sacrificing spatial reuse and yields lower average
 720 goodput. Besides the simulation results shown in this paper, we have also vali-
 dated the ASCA algorithm using channel counts up to 12 and the observations
 are similar to those using three available channels in this paper. This proves
 that the ASCA algorithm effectively solves flow starvation and improves the
 overall system fairness.

725 6. Conclusions

In this paper, we investigate how existing interference models influence the
 interference set selection in CA algorithms and network fairness in WMNs.
 With numerous simulation results, we found that the interference set selection
 strategies used by existing CA algorithms only consider the local interference
 730 among adjacent links and lack the consideration of global interference between
 border links and middle links. Hence, CA algorithms using these interference
 set selection strategies fail to prevent flow starvation and yield poor fairness.

We design a novel interference model that accounts for both global and
 local interference that goes beyond local interference. The newly proposed
 735 ASCA algorithm utilises this novel interference model that takes into account
 global and local interference in selecting interference sets. Moreover, the ASCA
 algorithm formulates the fairness among global interference sets as an ILP
 problem. Simulation results show that the ASCA algorithm effectively pre-
 vents flow starvation and achieves better fairness compared to the clique-based
 740 CA algorithm using existing interference models. In the future, we will study
 multi radio extensions for ASCA and explore multi-objective optimisation to
 achieve desired fairness and average goodput for planning WMNs.

References**References**

- 745 [1] I. F. Akyildiz, X. Wang, W. Wang, Wireless mesh networks: A survey, *Computer Networks*, Elsevier 47 (4) (2005) 445–487.
- [2] E. Hossain, K. K. Leung, *Wireless mesh networks: architectures and protocols*, Springer, 2007.
- [3] D. Benyamina, A. Hafid, M. Gendreau, Wireless mesh networks design—a
750 survey, *IEEE Communications Surveys & Tutorials* 14 (2) (2012) 299–310.
- [4] X. Fang, S. Misra, G. Xue, D. Yang, The new and improved power grid: A survey, *IEEE Communications Surveys Tutorials* 14 (4) (2012) 944–980.
- [5] R. Ma, H. H. Chen, Y. R. Huang, W. Meng, Smart grid communication: Its challenges and opportunities, *IEEE Transactions on Smart Grid* 4 (1)
755 (2013) 36–46.
- [6] S. Huaizhou, R. V. Prasad, E. Onur, I. Niemegeers, Fairness in wireless networks: Issues, measures and challenges, *IEEE Communications Surveys & Tutorials* 16 (1) (2014) 5–24.
- [7] P. Pathak, R. Dutta, A survey of network design problems and joint design
760 approaches in wireless mesh networks, *IEEE Communications Surveys Tutorials* 13 (3) (2011) 396–428.
- [8] R. H. Khan, J. Y. Khan, A comprehensive review of the application characteristics and traffic requirements of a smart grid communications network, *Computer Networks*, Elsevier 57 (3) (2013) 825–845.
- 765 [9] J. Kim, D. Kim, K.-W. Lim, Y.-B. Ko, S.-Y. Lee, Improving the reliability of IEEE 802.11 s based wireless mesh networks for smart grid systems, *Journal of Communications and Networks*, IEEE 14 (6) (2012) 629–639.

- [10] D. Benyamina, A. Hafid, M. Gendreau, J. Maureira, et al., On the design of reliable wireless mesh network infrastructure with qos constraints, *Computer Networks*, Elsevier 55 (8) (2011) 1631–1647.
- [11] I. Malanchini, S. Valentin, O. Aydin, Wireless resource sharing for multiple operators: Generalization, fairness, and the value of prediction, *Computer Networks*, Elsevier 100 (2016) 110–123.
- [12] Z. Wu, Y. H. Hu, How many wireless resources are needed to resolve the hidden terminal problem?, *Computer Networks*, Elsevier 57 (18) (2013) 3987–3996.
- [13] C. Hua, R. Zheng, On link-level starvation in dense 802.11 wireless community networks, *Computer Networks*, Elsevier 54 (17) (2010) 3159–3172.
- [14] M. Garetto, T. Salonidis, E. W. Knightly, Modeling per-flow throughput and capturing starvation in CSMA multi-hop wireless networks, *IEEE/ACM Transactions on Networking (ToN)* 16 (4) (2008) 864–877.
- [15] C. Hua, R. Zheng, Starvation modeling and identification in dense 802.11 wireless community networks, in: *Proceedings of the 27th IEEE Conference on Computer Communications (INFOCOM)*, Phoenix, AZ, USA, 2008, pp. 1022–1030.
- [16] A. Margolis, R. Vijayakumar, S. Roy, Modelling throughput and starvation in 802.11 wireless networks with multiple flows, in: *Proceedings of the IEEE Global Telecommunications Conference (GLOBECOM)*, LA, USA, 2007, pp. 5123–5127.
- [17] M. Durvy, O. Dousse, P. Thiran, Border effects, fairness, and phase transition in large wireless networks, in: *Proceedings of the 27th IEEE Conference on Computer Communications (INFOCOM)*, Phoenix, AZ, USA, 2008, pp. 601–609.
- [18] Y. Qu, B. Ng, W. K. G. Seah, A goodput distribution model for IEEE 802.11 wireless mesh networks, in: *Proceedings of the IEEE 34th In-*

ternational Performance Computing and Communications Conference (IPCCC), Nanjing, China, 2015, pp. 1–8.

- [19] M. W. Lee, G. Hwang, S. Roy, Performance modeling and analysis of IEEE 802.11 wireless networks with hidden nodes, in: Proceedings of the 16th ACM International Conference on Modeling, Analysis and Simulation of Wireless and Mobile Systems (MSWiM), ACM, Barcelona, Spain, 2013, pp. 135–142.
- [20] K. Jamshaid, P. A. Ward, M. Karsten, Mechanisms for centralized flow rate control in 802.11-based wireless mesh networks, *Computer Networks*, Elsevier 56 (2) (2012) 884–901.
- [21] K. Jamshaid, P. Ward, M. Karsten, B. Shihada, The efficacy of centralized flow rate control in 802.11-based wireless mesh networks, *EURASIP journal on Wireless Communications and Networking* 2013 (1) (2013) 163.
- [22] S. Rangwala, R. Gummadi, R. Govindan, K. Psounis, Interference-aware fair rate control in wireless sensor networks, in: *ACM SIGCOMM Computer Communication Review*, Vol. 36, ACM, 2006, pp. 63–74.
- [23] F. Nawab, K. Jamshaid, B. Shihada, P.-H. Ho, MAC-layer protocol for TCP fairness in wireless mesh networks, in: Proceedings of the 1st International Conference on Communications in China (ICCC), IEEE, 2012, pp. 448–453.
- [24] B. Bakhshi, S. Khorsandi, A maximum fair bandwidth approach for channel assignment in wireless mesh networks, in: Proceedings of Wireless Communications and Networking Conference (WCNC), IEEE, 2008, pp. 2176–2181.
- [25] B. Bakhshi, S. Khorsandi, On the performance and fairness of dynamic channel allocation in wireless mesh networks, *International Journal of Communication Systems*, Wiley Online Library 26 (3) (2013) 293–314.

- [26] M. Jahanshahi, M. Dehghan, M. R. Meybodi, A mathematical formulation for joint channel assignment and multicast routing in multi-channel multi-radio wireless mesh networks, *Journal of Network and Computer Applications*, Elsevier 34 (6) (2011) 1869–1882. 825
- [27] X. Lin, S. B. Rasool, Distributed and provably efficient algorithms for joint channel-assignment, scheduling, and routing in multichannel ad hoc wireless networks, *IEEE/ACM Transactions on Networking (TON)* 17 (6) (2009) 1874–1887. 830
- [28] N.-S. Vo, M.-H. Nguyen, D.-B. Ha, D.-T. Huynh, Joint distortion aware opportunistic routing and transmission rate assignment for video streaming over wireless mesh networks, in: *Proceedings of the International Conference on Computing, Management and Telecommunications (ComMan-Tel)*, IEEE, 2013, pp. 230–234. 835
- [29] J. Wellons, Y. Xue, The robust joint solution for channel assignment and routing for wireless mesh networks with time partitioning, *Ad Hoc Networks*, Elsevier 13 (2014) 210–221.
- [30] A. A. Franklin, V. Bukkapatanam, C. Murthy, On the end-to-end flow allocation and channel assignment in multi-channel multi-radio wireless mesh networks with partially overlapped channels, *Computer Communications*, Elsevier 34 (15) (2011) 1858–1869. 840
- [31] B. Bakhshi, S. Khorsandi, A. Capone, On-line joint QoS routing and channel assignment in multi-channel multi-radio wireless mesh networks, *Computer Communications*, Elsevier 34 (11) (2011) 1342–1360. 845
- [32] W. Si, S. Selvakennedy, A. Y. Zomaya, An overview of channel assignment methods for multi-radio multi-channel wireless mesh networks, *Journal of Parallel and Distributed Computing*, Elsevier 70 (5) (2010) 505–524.
- [33] A. A. Al Islam, M. J. Islam, N. Nurain, V. Raghunathan, Channel assign-

- 850 ment techniques for multi-radio wireless mesh networks: A survey, *IEEE Communications Surveys & Tutorials* 18 (2) (2016) 988–1017.
- [34] Y. Qu, B. Ng, W. Seah, A survey of routing and channel assignment in multi-channel multi-radio WMNs, *Journal of Network and Computer Applications*, Elsevier 65 (C) (2016) 120–130.
- 855 [35] X. Chen, J. Xu, W. Yuan, W. Liu, W. Cheng, Channel assignment in heterogeneous multi-radio multi-channel wireless networks: A game theoretic approach, *Computer Networks*, Elsevier 57 (17) (2013) 3291–3299.
- [36] V. Ramamurthi, A. S. Reaz, D. Ghosal, S. Dixit, B. Mukherjee, Channel, capacity, and flow assignment in wireless mesh networks, *Computer Networks*, Elsevier 55 (9) (2011) 2241–2258.
- 860 [37] Y. Qu, B. Ng, H. Yu, Anti-starvation channel assignment with global conflict set selection in IEEE 802.11 WMNs, in: *Proceedings of the 12th ACM Symposium on QoS and Security for Wireless and Mobile Networks (Q2SWinet)*, Malta, 2016, pp. 103–110.
- 865 [38] P. Dutta, S. Kalyanraman, A Classification Framework for Scheduling Algorithms in Wireless Mesh Networks, *IEEE Communications Survey & Tutorials* 15 (1) (2013) 199–222.
- [39] Y. Peng, Y. Yu, L. Guo, D. Jiang, Q. Gai, An efficient joint channel assignment and QoS routing protocol for IEEE 802.11 multi-radio multi-channel wireless mesh networks, *Journal of Network and Computer Applications*, Elsevier 36 (2) (2013) 843–857.
- 870 [40] B. Das, S. Roy, Load balancing techniques for wireless mesh networks: A survey, in: *International Symposium on Computational and Business Intelligence (ISCBI)*, IEEE, 2013, pp. 247–253.
- 875 [41] A. Raniwala, K. Gopalan, T.-c. Chiueh, Centralized channel assignment and routing algorithms for multi-channel wireless mesh networks, *ACM*

SIGMOBILE Mobile Computing and Communications Review 8 (2) (2004)
50–65.

[42] M. Kodialam, T. Nandagopal, Characterizing the capacity region in multi-
880 radio multi-channel wireless mesh networks, in: Proceedings of the 11th
annual international conference on Mobile computing and networking
(MobiCom), ACM, Cologne, Germany, 2005, pp. 73–87.

[43] S. Avallone, I. F. Akyildiz, A channel assignment algorithm for multi-radio
wireless mesh networks, *Computer Communications*, Elsevier 31 (7)
885 (2008) 1343–1353.

[44] S. Avallone, G. Stasi, A. Kessler, A traffic-aware channel and rate reassign-
ment algorithm for wireless mesh networks, *IEEE Transactions on Mobile
Computing* 12 (7) (2013) 1335–1348.

[45] X. Li, J. Wu, S. Lin, X. Du, Channel switching control policy for wireless
890 mesh networks, *Journal of Parallel and Distributed Computing*, Elsevier
72 (10) (2012) 1295–1305.

[46] S. M. Das, H. Pucha, D. Koutsonikolas, Y. C. Hu, D. Peroulis, DMesh: in-
corporating practical directional antennas in multichannel wireless mesh
networks, *IEEE Journal on Selected Areas in Communications* 24 (11)
895 (2006) 2028–2039.

[47] A. H. M. Rad, V. W. Wong, Joint optimal channel assignment and conges-
tion control for multi-channel wireless mesh networks, in: Proceedings of
IEEE International Conference on Communications (ICC), Vol. 5, Istanbul,
Turkey, 2006, pp. 1984–1989.

900 [48] V. Gardellin, S. K. Das, L. Lenzini, C. Cicconetti, E. Mingozzi, G-PaMeLA:
A divide-and-conquer approach for joint channel assignment and routing
in multi-radio multi-channel wireless mesh networks, *Journal of Parallel
and Distributed Computing*, Elsevier 71 (3) (2011) 381–396.

- [49] M. Alicherry, R. Bhatia, L. E. Li, Joint channel assignment and routing for
905 throughput optimization in multi-radio wireless mesh networks, in: Proceedings of the 11th annual international conference on Mobile computing and networking (MobiCom), ACM, Cologne, Germany, 2005, pp. 58–72.
- [50] F. Martignon, S. Paris, I. Filippini, L. Chen, A. Capone, Efficient and
910 truthful bandwidth allocation in wireless mesh community networks, IEEE/ACM Transactions on Networking 23 (1) (2015) 161–174.
- [51] K. Xing, X. Cheng, L. Ma, Q. Liang, Superimposed code based channel
assignment in multi-radio multi-channel wireless mesh networks, in: Proceedings of the 13th annual ACM international conference on Mobile computing and networking (MobiCom), Montreal, Quebec, Canada, 2007, pp.
915 15–26.
- [52] J. Wang, Z. Wang, Y. Xia, H. Wang, A practical approach for channel assignment in multi-channel multi-radio wireless mesh networks, in: Proceedings of the 4th IEEE International Conference on Broadband Communications, Networks and Systems (Broadnets), NC, USA, 2007, pp. 317–
920 319.
- [53] M. Shin, S. Lee, Y.-a. Kim, Distributed channel assignment for multi-radio wireless networks, in: Proceedings of the IEEE International Conference on Mobile Ad Hoc and Sensor Systems (MASS), Vancouver, BC, Canada, 2006, pp. 417–426.
- 925 [54] A. U. Chaudhry, N. Ahmad, R. H. Hafez, Improving throughput and fairness by improved channel assignment using topology control based on power control for multi-radio multi-channel wireless mesh networks, EURASIP Journal on Wireless Communications and Networking, Elsevier 2012 (1) (2012) 1–25.
- 930 [55] S. Kim, J. Cha, J. Ma, Interference-aware channel assignments with seamless multi-channel monitoring in wireless mesh networks, in: Proceedings

of the IEEE International Conference on Communications (ICC), Dresden, Germany, 2009, pp. 1–6.

- [56] R. Huang, S. Kim, C. Zhang, Y. Fang, Exploiting the capacity of multichannel multiradio wireless mesh networks, *IEEE Transactions on Vehicular Technology* 58 (9) (2009) 5037–5047.
- [57] M. Li, Y. Feng, Design and implementation of a hybrid channel-assignment protocol for a multi-interface wireless mesh network, *IEEE Transactions on Vehicular Technology* 59 (6) (2010) 2986–2997.
- [58] P. Kyasanur, N. H. Vaidya, Routing and link-layer protocols for multi-channel multi-interface ad hoc wireless networks, *ACM SIGMOBILE Mobile Computing and Communications Review* 10 (1) (2006) 31–43.
- [59] A. Brzezinski, G. Zussman, E. Modiano, Enabling distributed throughput maximization in wireless mesh networks: a partitioning approach, in: *Proceedings of the 12th annual international conference on Mobile computing and networking (MobiCom)*, ACM, CA, USA, 2006, pp. 26–37.
- [60] J. W.-T. Chan, F. Y. L. Chin, D. Ye, Y. Zhang, Absolute and Asymptotic Bounds for Online Frequency Allocation in Cellular Networks, *Algorithmica*, Springer 58 (2) (2010) 498–515.
- [61] G. Christodoulou, K. Ligett, E. Pyrga, Contention Resolution under Selfishness, *Algorithmica*, Springer 70 (4) (2014) 675–693.
- [62] A. Mishra, S. Banerjee, W. Arbaugh, Weighted coloring based channel assignment for WLANs, *ACM SIGMOBILE Mobile Computing and Communications Review* 9 (3) (2005) 19–31.
- [63] A. U. Chaudhry, R. H. Hafez, J. W. Chinneck, On the impact of interference models on channel assignment in multi-radio multi-channel wireless mesh networks, *Ad Hoc Networks*, Elsevier 27 (2015) 68–80.

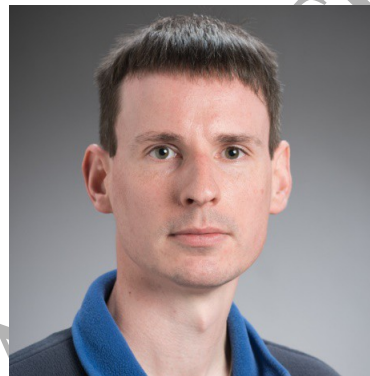
- [64] A. Iyer, C. Rosenberg, A. Karnik, What is the right model for wireless channel interference?, *IEEE Transactions on Wireless Communications* 8 (5) (2009) 2662–2671. 960
- [65] B. S. Chlebus, D. R. Kowalski, T. Radzik, Many-to-Many Communication in Radio Networks, *Algorithmica*, Springer 54 (1) (2009) 118–139.
- [66] I. C. S. L. M. S. Committee, et al., IEEE 802.11: WIRELESS LAN medium access control and physical layer specifications (1999).
- [67] A. Goldsmith, *Wireless communications*, Cambridge university press, 2005. 965
- [68] J. Tang, G. Xue, W. Zhang, Interference-aware topology control and QoS routing in multi-channel wireless mesh networks, in: *Proceedings of the 6th ACM international symposium on Mobile ad hoc networking and computing*, 2005, pp. 68–77. 970
- [69] K. Xu, M. Gerla, S. Bae, How effective is the IEEE 802.11 RTS/CTS handshake in ad hoc networks, in: *Proceedings of the Global Telecommunications Conference (GLOBECOM)*, Vol. 1, IEEE, Taipei, Taiwan, 2002, pp. 72–76.
- [70] P. N. D. Bukh, R. Jain, *The art of computer systems performance analysis, techniques for experimental design, measurement, simulation and modeling* (1992). 975
- [71] Y. Qu, B. Ng, The effect of carrier sensing mechanisms on wireless mesh network goodput, in: *Proceedings of International Telecommunication Networks and Applications Conference (ITNAC)*, IEEE, Sydney, Australia, 2015, pp. 106–113. 980
- [72] H. W. Lenstra Jr, Integer programming with a fixed number of variables, *Mathematics of operations research*, INFORMS 8 (4) (1983) 538–548.



Ying has been working towards the Ph.D. degree in the area of communication and networking at Victoria University of Wellington, New Zealand since 2013. Her main research interests are performance modeling and channel assignment in wireless mesh networks.



Bryan completed his PhD (2010) in the area of communication and networking. He held teaching & research positions in Malaysia and France in addition to attachments to commercial research laboratories Intel, Motorola, Panasonic and Orange Labs. His research interest include performance analysis of communication networks, modelling networking protocols and software defined networking.



Michael is a Lecturer in Software Engineering at Victoria University of Wellington who works primarily on programming languages, and their algorithms and education.